Cr oxide coated woodland camouflage textiles for protection of defense target signature in UV-Visible-IR spectrum opposing of hyperspectral and digital imaging

Md. Anowar Hossain (engr.anowar@yahoo.com)
RMIT University

Article

Keywords:

Posted Date: January 4th, 2023

DOI: https://doi.org/10.21203/rs.3.rs-2298847/v1

Abstract

The chromatic intensity and thermal mechanism are vital segment for protection of military target in ultraviolet (UV)-visible (Vis)-infrared (IR) imaging. Defense operations need to confront with UV-Vis-IR imaging to distinguish/conceal the target from combat background (CB). The key purpose of this experimentation is to develop the imaging and optical intensity concepts of chromatic appearance for concealment, detection, recognition, and identification (CDRI) of Cr oxide coated target signature against hyperspectral and digital camera imaging in UV-Vis-IR optical signal. Chromatic intensity of Cr oxide formulated polyamide 6,6 (PA-6,6) fabric was examined by Vis-IR-hyperspectral imaging (HSI) in 400 nm, 500 nm, 600 nm, 700 nm, 1000 nm, 1300 nm, 1600 nm, 1900 nm, 2200 nm, 2500 nm. UV-Vis-IR-HSI has been experimented by international commission on illumination (CIE); red-green-blue standardized color scale for concealment and detection in UV-Vis-IR optical ranges. Concealment of target signature was observed in 400 nm, 500 nm, 600 nm, 700 nm, 2200 nm and 2500 nm when Cr oxide coated PA-6,6 fabric was scanned in 22,948 μs (microsecond)-Vis-HSI and 10,500 μs-IR-HSI. The optical reflection and CIE-chromaticity of Australian grass, *Bothriochloa Pertusa,* woodland CB and Cr oxide coated PA-6,6 fabric have been observed similarity under UV-Vis-IR optical assessment.

Introduction

Ultraviolet (UV)-visible (Vis)-infrared (IR) reflection of chromium oxide has similarity with Australian grass, *Bothriochloa Pertusa;* a common material of woodland combat background (CB). Cr pigment shows higher absorbance in Vis ranges and maximum reflection in IR ranges. For woodland camouflage textiles, the imaging properties of woodland CB should be matched with the reflection profile of pigment coated textiles. Generally green pigment, Cr oxide is considered as 'synthetic chlorophyll' which is responsible for symmetric chromatic profile of green plants of woodland CB[1–3]. Camera imaging and intensity of target signature is related to photon movements. Photon is massless, chargeless; moves at the speed of light; symbolized by $E = mc^2$ and $E = hv = hc/$, photon energy forms imaging scanned by digital camera or hyperspectral camera; carries energy from target signature to the light source on its intensity and generates imaging of target object against CB[4, 5]. The distribution of frequencies and intensities of camera lens allows to generate image formation. Travelling time of photon between target signature and camera light source can alter the target imaging[6]. Hyperspectral versus textile imaging is a new concept of concealment, detection, recognition and identification (CDRI) applications for development of camouflage textiles against CB. Therefore, camouflage assessment technique and right camouflage materials identification may protect the special force of defense for concealment of target signature against high-performance imaging.

Experimental Design Of Materials And Methodology

Cr oxide coating on PA-6,6 fabric. 130 GSM polyamide 6,6 (PA-6,6) fabric was selected for this experimentation. Cr oxide was used as alternative of synthetic chlorophyl; chromacryl, polyurethane based tubicoat (PU-tubicoat)[7], a combination of thermoplastic polyurethane (TPU) and N,N-dimethylformamide (DMF) were experimented as synthetic binder; an Australia based supplier. A coating paste was prepared with Cr oxide and chromacryl/PU-tubicoat binder/TPU-DMF in the ratio of 1:1 and coated with different techniques. Machine coating, scrabber coating and dip coating method was followed for making a thin layer of Cr oxide on PA-6,6 fabric surface in sample development stage.

Sample preparation for hyperspectral scanning. A “red leaf marker 707” made in Japan was used for reddish tone ‘circular area’ target detection and a “good luck marker” made in Bangladesh was implemented for black tone ‘circular area’ target marking on uncoated PA-6,6 fabric. The color properties of selected marker were unknown. Cotton yarn stitched-two-layer PA-6,6 coated and uncoated fabric were used for hyperspectral scanning. Cotton yarn stitched-two-layer PA-6,6 uncoated and cotton dyed fabric was also designed and standardized for hyperspectral scanning.

Sample collection and preparation of Australian grass, Bothriochloa Pertusa**as specified sample of woodland CB.** A formal identification of selected Australian grass, *Bothriochloa Pertusa* as specified sample of woodland CB by looking foremost properties such as aesthetic appearance, root and branches, leaf shape and size, leaf arrangement; and followed general guideline of sample collection applied for this experimentation[8]. Average height of grass sample was selected for this experimentation. Australian grass, *Bothriochloa Pertusa* was used for reflection measurement of woodland CB for comparison with synthetic chlorophyl coated PA-6,6 fabric. For imaging measurement of *Bothriochloa Pertusa*, fresh green grasses were cut, washed, water extracted and dried at 40°C, 30 minutes and tested after 4 hours. Fresh green grasses were collected from Princes Park, Melbourne during September-November 2021. Fresh grasses were dried with natural illumination, sun light at window around three months during September-November 2021.

Exemption note of Australian grass, Bothriochloa Pertusa **collection and approval for assessment as woodland CB material.** A minimum amount (around 200 gm) of *Bothriochloa Pertusa* including ‘agricultural waste’[9] were collected from non-commercial sources applied for non-commercial application. All experiments were conducted with accordance to relevant regulations and guidelines under academic platform of camouflage research. Therefore, permission of *Bothriochloa Pertusa* sample collection is not required. This exemption is supported by ‘3.1.2, assessment requirement’ for collection of *Bothriochloa Pertusa* sample quoted as below, registered research located in Australia:

“A permit is not required to collect native plant material from private land, unless: the species for collection are listed threatened species or form part of a threatened ecological community under the environment protection and biodiversity conservation (EPBC) Act, under such circumstances a Commonwealth permit may be required”[10].

Imaging of scanning electron microscopy (SEM). A table microscope SEM machine was used for electron imaging. TM4000/TM4000Plus, Hitachi, Japan and SC7620 sputter coater, Quorum, UK were used as set up of SEM. 100 magnification SEM imaging was captured by 15KV power selection. An auto contrast imaging was generated to magnify the Cr oxide coated PA-6,6 fabric surface for comparison with uncoated PA-6,6 fabric.

Imaging/scanning method of hyperspectral camera in IR spectrum, 1000–2500 nm. Figure 1, hyperspectral camera, SWIR-384, Raymax Application Ltd. was used for testing of CDRI. The lens was 30 cm focal lens and the working distance between camera and textile sample was kept 208 millimetre. Every scanning captured full wavelength of spectrum. Hyperspectral camera captured 288 band in full wavelength of spectrum, shown in supporting information, Table SI 1. The camera was calibrated to measure 288 bands in short wavelength region. Closest band of 1000 nanometer (nm) (1000.292), 1300 nm (1301.079, 1600 nm (1600.866), 1900 nm (1900.653), 2200 nm (2200.441), 2500 nm (2500. 228) were recorded for jpeg images of target signature and spectral data information. Each scan was captured including all band. Each pixel captured including the full wavelength of spectrum[11]. There was one-line time frame taken every 30,000 microseconds (μs) under a stage linear speed of approximately o.822 cm/sec. Within the time frame of hyperspectral camera, the integration time was adjusted in two different μs for correct imaging signal of PA-6,6 fabric. The timeframe 7,500 μs was scanned for imaging of PA-6,6 uncoated fabric denoted as PA-6,6 fabric sample-1 and PA-6,6 fabric sample-2, if 10,500 μs was used for Cr oxide uncoated PA-6,6 fabric, too many photons would reach the sensor and the signal would be saturated. 10,500 μs timeframe was also selected for imaging of Cr oxide coated PA-6,6 fabric, PA-6,6 fabric sample-3 and PA-6,6 fabric sample-4 when using 7,500 μs, the Cr oxide coated fabric was remarked as almost invisible, it was not captured enough photons to the hyperspectral camera sensor, and the signal would be too low to identify target object (TOB). The signal level for each wavelength on the images is displayed according to international commission on illumination (CIE); red, green, blue (RGB) color scale where the intensity of blue hue demonstrates minimum photon signal and the intensity of red signifies maximum photon response to the sensor of hyperspectral camera, Fig. 1. Each image and selection of pixel was focused for high contrast. The aperture was expanded for more photon to reach the sample and capturing correct signal to hyperspectral camera. Sensor of hyperspectral camera was adjusted with aperture duration, 10,500 μs to obtain strong enough photon and maximum pixel saturation from Cr oxide coated textiles. Hyperspectral camera room was kept in little darker to reduce possible interference with data acquisition. The temperature of scanning moment was kept at room temperature around 20˚C. Hyperspectral imaging (HSI) was captured around 45˚ angles to the fabric surface[12–14].

Imaging/scanning method of hyperspectral camera in Vis spectrum, 400–700 nm. In general, similar observation of IR-HSI was followed for Vis-TOB. This scanning was evaluated by hyperspectral camera at 400 nm, 500 nm, 600 nm and 700 nm. HySpex VNIR-1800 was used with 30 cm focal length, the integration time was applied 22,948 μs for every sample measurement. A base fabric PA-6,6; a red color standardized cotton fabric; and Cr oxide coated and padded PA-6,6 fabric were scanned with Vis-HSI. A standardized red color cotton fabric was used for comparison of reddish tone intensity with Cr oxide coated and uncoated PA-6,6 fabric in Vis-HSI[12].

Figure 1, HSI was captured by line scanning method of hyperspectral camera. A middle line absorption value was implemented for generation of graphical correlation between absorption versus wavelength at 1000 nm, 1300 nm, 1600 nm, 1900 nm, 2200 nm, 2500 nm. The whole absorption value of PA-6,6 fabric sample-01, 02, 03, 04 scanned by hyperspectral camera at 1000 nm, 1300 nm, 1600 nm, 1900 nm, 2200 nm, 2500 nm have been shown in supporting information Table SI 2–25.

Vis-infrared (IR) camera scanning method. Assessment of Vis-IR capturing was followed by a standard equation for the measurement of photonic response through imaging signal of Cr oxide coated fabric against woodland CB, *Bothriochloa Pertusa*.

D/S = SSR

D = distance from the camera to the target

S = smallest target dimension of OB

SSR = spot size ratio

Measurement was executed in D65-UV background 'light box' under protection of outside interference of light. FLIR T440 thermal imaging camera, USA; IR lens, focal length (F) = 18 millimetre; calibrated by national institute of standards and technology (NIST), USA, IR range: 900-14000 nm (approximately) was used for this experimentation of FLIR imaging. The standardized reflectance of black, green, and white background was used for UV-Vis-IR optical assessment[15]. Figure 2 shows the standardized chromatic value experimented for optical assessment of UV-Vis-IR-TOB-CB[14].

A field trialling of Cr oxide coated PA-6,6 fabric was performed against woodland CB at grass ground, RMIT University Campus under natural illumination, sunlight[16, 17]. A combined 'dry grass' and 'green grass' of woodland CB was selected for field trialling. The distance between target coated fabric and FLIR camera was kept 18 inches. Practically there is possible deviation between FLIR captured temperature and original temperature of captured environment, although FLIR captured temperature was recorded and standardized for imaging properties.

Results And Discussion

Figure 3–11; in general, it is being clearly signified and correlated that temperature of target signature, Cr oxide coated textiles and woodland CB materials influence the energy state (E) at UV-Vis-IR spectrum which changes the vibrational state from minimum (19˚C) to maximum (60˚C) level; hence the chromatic intensity of UV-Vis-IR/electron imaging altered through energy deviation as per established quantum mechanics of $E = mc^2$ and $E = hv = hc/$ [4, 5]. Therefore, The mechanism of absorption, transmission and reflection of PA-6,6-Cr oxide formulated fabric against woodland CB has been instigated for optical assessment of camouflage textiles in UV-Vis-IR spectrum[16].

Imaging of SEM. Figure 3b, Cr oxide-PU has been well cemented with PA-6,6 fabric surface. Because of white chromatic hue, PU presency has been depicted on PA-6,6 fabric surface but the maximum percentage of PU has been overlapped by the Cr oxide deposition. The imaging of electron microscopy has been confirmed the chromatic replacement when PA-6,6 fabric was coated with Cr oxide. The electron imaging has also been signified the lower reflection of Cr oxide coated fabric due to darker chromatic hue. The electron imaging of Cr oxide coated fabric has been assumed similarity with the electron imaging of woodland CB material, *Bothriochloa Pertusa*[18]. Therefore, the existing Cr oxide molecule has been approached to have a tendency of chromatic matching with woodland CB material, *Bothriochloa Pertusa*.

Target assessment of PA-6,6 fabric sample-01, 02, 03, 04; imaging phase-1 (Vis-HSI, 400–700 nm, optical assessment)

Target assessment of PA-6,6 fabric sample-01, 02, 03, 04; imaging phase-1 (Vis-HSI, optical assessment). Figure 4a, 4f are the uncoated PA-6,6 fabric. Figure 4k has been shown cotton fabric to show the reddish intensity for comparison in Vis-HSI. Figure 4p and 4u are the Cr oxide coated PA-6,6 fabric under two different formulations of coating. Figure 4a, back layer of PA-6,6 fabric was marked 'circular area' with the combination of black and red color. Figure 4f, front layer of PA-6,6 fabric was marked 'circular area' with the combination of black and red color. Figure 4k, back layer of PA-6,6 fabric was marked 'circular area' with the combination of black and red color. Similarly, Fig. 4p, 4u; back layer of PA-6,6 fabric was marked 'circular area' with the combination of black and red color. Figure 4b, 4g, 4i, 4q, 4v are shown as HSI at 400 nm. Figure 4c, 4h, 4m, 4r, 4w are remarked as HSI at 500 nm. Figure 4d, 4i, 4n, 4s, 4x are signified the HSI at 600 nm. Figure 4e, 4j, 4o, 4t, 4y are identified as HSI at 700 nm. In Vis-HSI, the intensity of black and red, 'circular area' was detected at 400 nm, Fig. 4b; 500 nm, Fig. 4c; 600 nm, Fig. 4d; and 700 nm Fig. 4e but the chromaticity was gradually declined from 400 nm to 700 nm, Fig. 4b-4c-4d-4e. Similarly, the intensity of black and red, 'circular area' was identified at 400 nm, Fig. 4g; 500 nm, Fig. 4h; 600 nm, Fig. 4i; and 700 nm Fig. 4j but the chromaticity response was gradually weakened from 400 nm to 700 nm, Fig. 4g-4h-4i-4j. A different chromaticity was visualized at 400 nm, Fig. 4g and 500 nm, Fig. 4h due to deviation of chromatic intensity. As PA-6,6 fabric has circular cross section, it may have reflection at different angle[1], the chromatic intensity of 'circular area' has also been scattered with background reflection. Hence, the intensity of uncoated PA-6,6 image was almost nil due to the chromaticity signal of Vis-HSI. Figure 4b-4c-4d-4e and 4g-4h-4i-4j; the intensity of black and red chromatic hue was comparatively higher in Vis-HSI, chromaticity assessment was classified on white background, uncoated PA-6,6 fabric. Figure 4o, the chromatic intensity of red background was also higher for standardized red color fabric at 700 nm. Figure 4q-4r-4s-4t and 4v-4w-4x-4y; the intensity of Cr oxide coated fabric was observed bluish chromatic hue when the Cr oxide was tended to higher in digital imaging, Fig. 4p, 4u. The intensity of back layer 'circular area' was completely nil due to chromaticity signal of Vis-HSI. The intensity of Cr element was completely nil due to minimum photonic response to hyperspectral sensor. Hence, the chromatic intensity of Cr oxide coated fabric was also invisible due to minimum photonic response to hyperspectral sensor. The 'circular mark' object was concealed due to greenish reflection of

Cr oxide coated fabric when the backside layer of Cr oxide coated fabric was also marked with ‘circular area’. Cr oxide coated fabric has been depicted less reflection to the hyperspectral camera sensor. Therefore, lower chromatic intensity of Cr oxide in Vis-HSI has been depicted, Cr oxide coated fabric was compared with woodland CB for next stage assessment of field trialling.

Target assessment on PA-6,6 fabric sample-01, imaging phase-2 (IR-HSI, 1000–2500 nm optical assessment). Figure 5, PA-6,6 fabric background shows minimum absorption in every spectrum from 1000 nm to 2500 nm. Absorption is higher at 2200 nm and 2500 nm and comparatively lower absorption is found at 1000–1900 nm which may signify the lowest reflection of PA-6,6 fabric at 2200 nm and 2500 nm, and comparatively higher reflection is recorded at 1000–1900 nm shown in Fig. 5a, 5b. A gradual declining of reflection has been depicted due to higher absorbency at 2500 nm and lower absorbency at 1000 nm, 1300 nm, 1600 nm, and 1900 nm. The reflection of chromatic hue of red and black circle has been found remarkable at 1000–1900 nm. The signified circle has been concealed at 2200 nm and 2500 nm due to minor photonic signal in IR-HSI. At 2500 nm, there is nil chromatic signal has been detected. It has been confirmed that PA-6,6 fabric and its remarked area of ‘circular mark’ has no identification at 2500 nm. Due to high reflection of PA-6,6 fabric, the reflection to the IR-HSI has been classified as concealed object from 1000 nm to 2500 nm. A scattered reflection of ‘reddish circle’ tone has been identified on the fabric surface from 1000 nm to 2200 nm due to deviation of photonic response. Circular reddish tone has been smashed with the base area of bluish tone due to movement of photonic responses in IR, but the ‘circular area’ of reddish tone is almost invisible. The intensity of black circle is gradually decreased from 1000 nm to 1900 nm. Furthermore, as surrounding area of fabric was stitched with 100% cotton yarn which is also illuminating as higher absorption, it seems a low reflection signal of cotton yarn in photonic response of IR-HSI.

Target assessment on PA-6,6 fabric sample-02, imaging phase-3 (IR-HSI, 1000–2500 nm optical assessment). Figure 6, black circle is identified at 1000 nm and concealed at 1300 nm, 1600 nm, 1900 nm, 2200 nm and 2500 nm. Absorption is gradually increased from 1000 nm to 2500 nm and sequentially it seems reflection remarkably decreases at 2500 nm. Red circle is scattered and smashed with the base area from 1000 nm to 2200 nm. A nil-reflection tendency has been remarked at 2500 nm. A gradual declining of reflection has been depicted due to higher absorbency at 2500 nm and lower at 1000 nm, 1300 nm, 1600 nm and 1900 nm.

Target assessment on Cr oxide coated PA-6,6 fabric sample-03, imaging phase-4 (IR-HSI, 1000–2500 nm optical assessment). Figure 7, Cr oxide coated fabric creates concealed of backside signature of black and red color, but the chromatic intensity of reddish signature is prominent from 1000 nm to 2200 nm. Due to lacking of reddish combination, the Cr oxide coated fabric is completely bluish at 2500 nm, it means the invisible surface of Cr oxide coated surface. A gradual declining of reflection has been depicted due to higher absorbency at 2500 nm and lower absorbency at 1000 nm, 1300 nm, 1600 nm, and 1900 nm.

Target assessment on Cr oxide coated PA-6,6 fabric sample-04, imaging phase-5 (IR-HSI, 1000–2500 nm optical assessment). Figure 8, black and red marked 'circular area' is completely concealed by the Cr oxide coated fabric. The tonal area of red circle has been scattered at 1000 nm, 1300 nm, 1600 nm, 1900 nm. There is no effect of black and red marked area at 2200 nm and 2500 nm. In general, a light greenish intensity has been observed at IR range, 1000–2500 nm due to chromatic intensity.

Figure 8, Cr oxide coated PA-6,6 background shows minimum absorption in every spectrum 1000 nm to 2500 nm. Absorption is higher at 2200 nm and 2500 nm and comparatively lower absorption is found at 1000–1900 nm which may signify the lowest reflection of PA-6,6 fabric at 2200 nm and 2500 nm; and oppositely highest reflection is recorded at 1000–1900 nm shown in Fig. 8a, 8b. A gradual declining of reflection has been depicted due to higher absorption at 2200 nm and 2500 nm and lower absorption at 1000 nm, 1300 nm, 1600 nm and 1900 nm. The reflection of chromatic hue of 'red and black circle' has found remarkable at 1000–1900 nm. The signified circle has been concealed at 2200 nm and 2500 nm due to minor photonic signal in IR-HSI. At 2500 nm, there is nil chromatic signal has been detected. It has been confirmed that PA-6,6 fabric and its remarked area has no identification at 2200 nm and 2500 nm. Due to high reflection of PA-6,6 fabric, the reflection to the IR-HSI has been classified as concealed object of 'circular area' from 1000 nm to 2500 nm. A scattered reflection of reddish circle tone has been identified on the fabric surface from 1000 nm to 1900 nm. As surrounding area of fabric was stitched with 100% cotton yarn which is also illuminating as higher absorption of HSI scanned line, it seems a low reflection signal of cotton yarn in IR-HSI, 1000–2500 nm.

Target assessment of Cr oxide coated PA-6,6 fabric against dry grass, woodland CB, Bothriochloa Pertusa **imaging phase-6 (digital imaging in UV-Vis-IR optical assessment).** Figure 9a, 9b; the chromatic intensity of dry grass, woodland CB has been found concealment effect under the optical assessment of D65-UV-Vis rather than exceptional at white background.

Figure 9c, 9d, 9e, 9f; under D65-IR optical assessment, TOB is detected as bluish chromatic hue due to deviation of dry grass reflection and synthetic chlorophyl/Cr oxide existing on PA-6,6 fabric surface but the chromatic intensity is almost similar. TOB has been found as concealed under low temperature at 19.3˚C, and increasing the temperature gradually differentiate the TOB and woodland CB material under D65 background at 25.5˚C, 29.4˚C and 57.3˚C. Figure 9g, 9h, 9i; similarly, TOB is concealed under low temperature at 20.3˚C; and the TOB is detected under high temperature at 42.7˚C and 56.6˚C under UV-IR lighting assessment.

Target assessment on Cr oxide coated PA-6,6 fabric against green grass, woodland CB, Bothriochloa Pertusa **imaging phase-7 (digital imaging in UV-Vis-IR optical assessment).**

Figure 10a shows Vis image of D65 background and Fig. 10b shows Vis image of UV background. Figure 10c, 10d, 10e shows IR image of D65 background at 30.7˚C, 57.2˚C, 60.9˚C. Figure 10f, 10g, 10h identifies IR image of UV background at 28.6˚C, 30.0˚C and 33.1˚C. Figure 10a, 10b; both D65-UV background appeared the chromatic matching with green grass background in Vis imaging. Figure 10c, 10d, 10e; Cr oxide coated PA-6,6 fabric shows the matching of chromatic appearance with woodland CB without color difference between TOB and CB material at different temperature of IR imaging in D65-UV background. In photochemical process, Cr is a major element of green grass in woodland CB. Hence, Cr is responsible for chromatic matching between woodland CB and Cr oxide coated PA-6,6 fabric. The concealment of Cr oxide coated fabric has been found prominent for application in UV-Vis-IR imaging.

Target assessment of Cr oxide coated PA-6,6 fabric against green grass woodland CB, Bothriochloa Pertusa, **imaging phase-8 (digital imaging in Vis-IR optical assessment), a field trialling.** Figure 11a denotes the Cr oxide coated PA-6,6 fabric, surrounded with uncoated PA-6,6 fabric, placed on grass surface, woodland CB. Figure 11b, grass surface generates yellowish and reddish chromaticity due to light reflection of soil background, a comparatively heated surface than grass. Similarly, Cr oxide coated PA-6,6 fabric shows yellowish and reddish color hue which is almost matching with the chromaticity of grass surface, woodland CB. Figure 11c, 11d the deviation of temperature, minimum temperature, maximum temperature influences the spot temperature captured by IR camera, it is also related to chromatic hue of black to white coordinates for concealment and detection of target signature.

Concluding Remarks

An application of synthetic chlorophyl on PA-6,6 fabric can be developed for woodland camouflage textiles against hyperspectral or digital imaging in UV-Vis-IR spectrum. Cr oxide coated fabric has been found suitability for concealment against Australian grass, *Bothriochloa Pertusa* due to existing elements of Cr in green grass although viewing geometry/sensor/illumination type of hyperspectral or digital camera may influence the chromatic and achromatic reflection on PA-6,6 fabric surface for CDRI versus optical assessment. It can be formulated that photon carries energy or momentum from PA-6,6 fabric surface to the camera lens and generates frequency for imaging. Therefore, the frequency vibrates the photo sensitive materials/sensor of hyperspectral camera which creates imaging of fabric surface. The direction of photon may be replaced/controlled by the Cr oxide modification of textile surface which can be matched with woodland CB. Furthermore, raw PA-6,6 fabric may also be used for design of parachute fabric of special team in defense. 100% uncolored PA-6,6 fabric may be camouflage at IR-HSI due to high reflection in selected range of scanning with HSI when the CB is sky. The patterning principle of parachute fabric can also be implemented by black patterning on PA-6,6 fabric for concealment in IR and recognition in Vis. Oppositely defense identification of target signature can be implemented by red patterning in Vis-IR-HSI.

Declarations

Declaration of conflicting interests

The author declared no potential conflicts of interest with respect to the research, authorship and/or publication of this article.

Funding

The author received no financial support for the research, authorship and/or publication of this article.

Data availability statement

All data generated or analyzed during this experimentation are included in supplementary information file; Table SI 1-25.

Acknowledgement

Author, Md. Anowar Hossain, PhD application ID: 2612540, PhD student ID: 3820066, Bangladeshi national ID: 19862692620993890; Lecturer (study leave), City University, Dhaka, Bangladesh acknowledges RMIT University and Australian government for funding through research training program (RTP) stipend scholarship. Author acknowledges to “Professor Lijing Wang” and “Emeritus Professor Robert Shanks”, School of Fashion and Textiles, RMIT University for their supervision works. Author also acknowledges to Dr. Cedric Chaminade, Technical Director/Physicist, Raymax Applications Ltd. for his scanning support of hyperspectral camera during COVID-19 restriction.

Open Researcher and Contributor ID (ORCID)

Md. Anowar Hossain: *https://orcid.org/0000-0003-2880-6287*

References

1. Gupta KK, Nishkam A and Kasturiya N. Camouflage in the Non-Visible Region. Journal of Industrial Textiles 2016; 31: 27–42. DOI: 10.1106/lmq5-x8lk-27rj-urpl.
2. Gao Y, Tang B, Ji G, et al. A camouflage coating with similar solar spectrum reflectance to leaves based on polymeric inorganic composite. Materials Research Express 2021; 8. DOI: 10.1088/2053-1591/ac04e7.
3. Jose S, Joshy D, Narendranatha SB, et al. Recent advances in infrared reflective inorganic pigments. Solar Energy Materials and Solar Cells 2019; 194: 7–27. DOI: 10.1016/j.solmat.2019.01.037.
4. Johansson I. Professor emeritus in philosophy, The Avogadro Constant, the Planck Constant, and the New SI (Metrological-philosophical reflections not submitted to any journal). In: Umeå University S, (ed.). Address: Virvelvindsvägen 4P, SE-222 27 Lund, Swedeningvar.johansson@philos.umu.se.
5. Tan YP. Fluorescence and Confocal Microscopy. Neurotransmitter Release and Uptake. 1997, pp.39–48.
6. New photon-counting camera captures 3D images with record speed and resolution. The Optical Society ScienceDaily,., 2020.
7. Hossain MA. Evaluation of Camouflage Coloration of Polyamide-6,6 Fabric by Comparing Simultaneous Spectrum in Visible and Near-Infrared Region for Defense Applications. In: Samanta AK (ed) *Colorimetry*. London, United Kingdom: IntechOpen, 2021, pp.1–22.

8. Hossain A. A Practical Guideline of Few Standardized Ready Made Shades of Natural Dyed Textiles. In: Samanta AK and Awwad NS (eds) *Chemistry and Technology of Natural and Synthetic Dyes and Pigments*. London, United Kingdom: IntechOpen, 2020, pp.151–170.
9. Linhares T and Amorim MTPd. Cotton Dyeing with Extract from Renewable Agro Industrial Bio-resources: A Step Towards Sustainability. In: Fangueiro R and Rana S (eds) *Natural Fibres: Advances in Science and Technology Towards Industrial Applications*. Rilem Bookseries, 2016.
10. Native Plant Material Collection Standard; Department of Environment and Heritage, Government of South Australia; National Parks and Wildlife Act, 1972. Science and Conservation Directorate Biodiversity Conservation Programs, 2007, p. 7/17.
11. Jianxin Z, Junkai W, Xudong H, et al. Multi-color measurement of printed fabric using the hyperspectral imaging system. Textile Research Journal 2020; 90: 1024–1037. DOI: 10.1177/0040517519883953.
12. Hossain MA. Adaptive Camouflage Textiles with Thermochromic Colorant and Liquid Crystal for Multidimensional Combat Background, a Technical Approach for Advancement in Defence Protection. American Journal of Materials Engineering and Technology 2021; 9: 31–47. DOI: 10.12691/materials-9-1-3.
13. Hossain A. Spectral simulation and method design of camouflage textiles for concealment of hyperspectral imaging in UV-Vis-IR against multidimensional combat background. The Journal of the Textile Institute 2021: 1–12. DOI: 10.1080/00405000.2022.2027074.
14. Hossain MA. *Basic Knowledge of Wet Processing Technology*. 140, Islamia Market, Nilkhet, Dhaka, Bangladesh: Rupok Publications; ISBN-978-984-35-2885-8 (printed copy), 2009.
15. O'Donnell C, Esquerre C, Downey G, et al. Use of spectral pre-processing methods to compensate for the presence of packaging film in visible–near infrared hyperspectral images of food products. Journal of Spectral Imaging 2010; 1: 10. DOI: 10.1255/jsi.2010.a1.
16. Hossain MA. Camouflage Assessment Of Aluminium Coated Textiles for Woodland and Desertland Combat Background in Visible and Infrared Spectrum under UV-Vis-IR Background Illumination. Defence Science Journal 2022; 72: 359–370. DOI: 10.14429/dsj.72.17731.
17. Hossain A. Concealment, Detection, Recognition, and Identification of Target Signature on Water Background under Natural Illumination. International Journal of Science and Engineering Investigations 2021; 10: 1–11.
18. Hossain A. Simulation of chromatic and achromatic assessments for camouflage textiles and combat background. Journal of Defense Modeling and Simulation: Applications, Methodology, Technology, 2021: 1–16. DOI: 10.1177/15485129211067759.

Figures

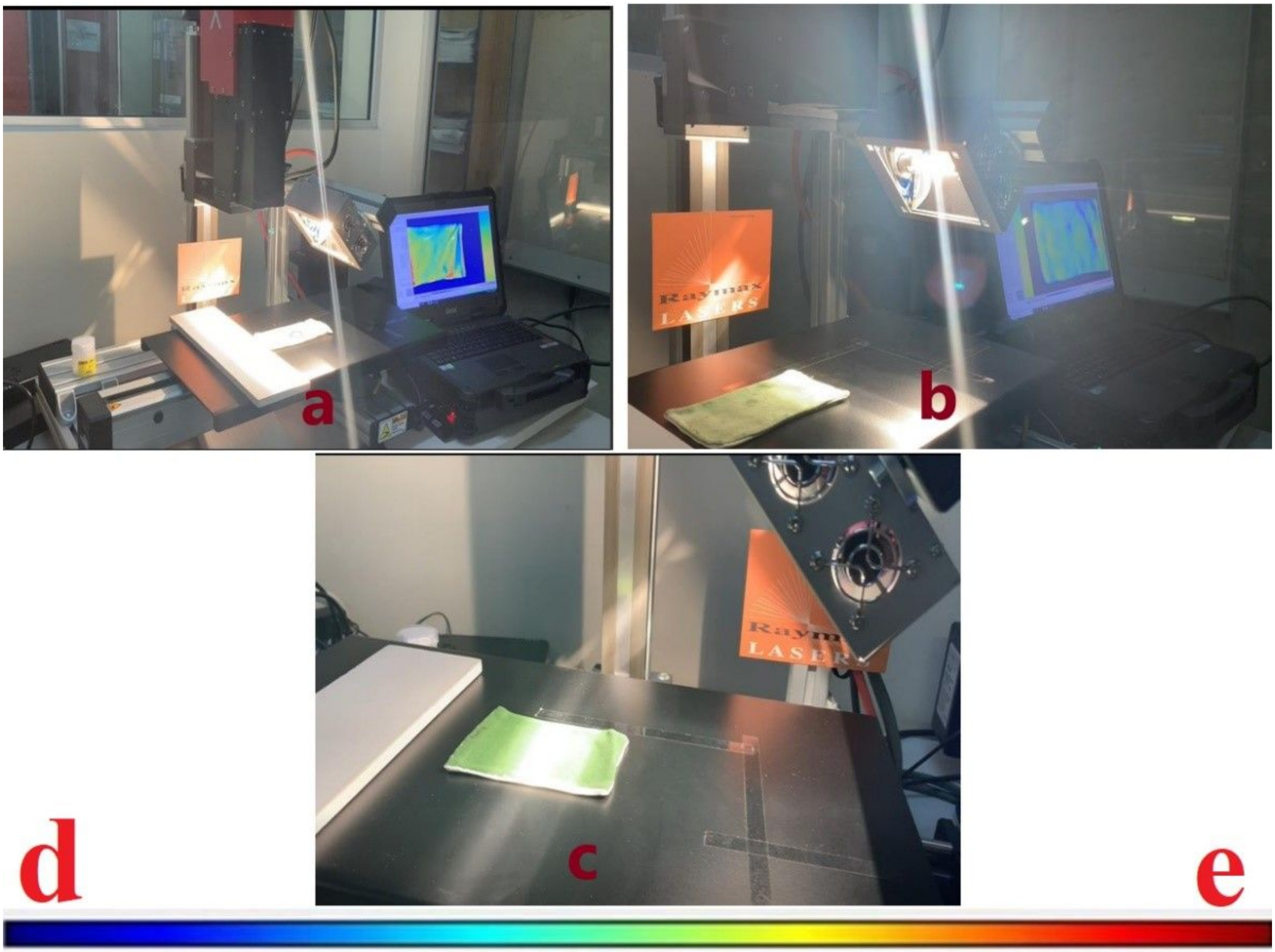

Figure 1

Hyperspectral camera setting and testing conditions of Cr oxide uncoated PA-6,6 fabric (a), coated PA-6,6 fabric (b, c) and standardized color scale blue to red (de).

Standard Tiles	L*	a*	b*
Green standard	52.56	-27.49	11.7
White standard	94.21	-1.4	0.57
Black standard	0.02	0	0

Figure 2

Standard tiles of black, green and white background (left) and its color combination of L*, a*, b* (right).

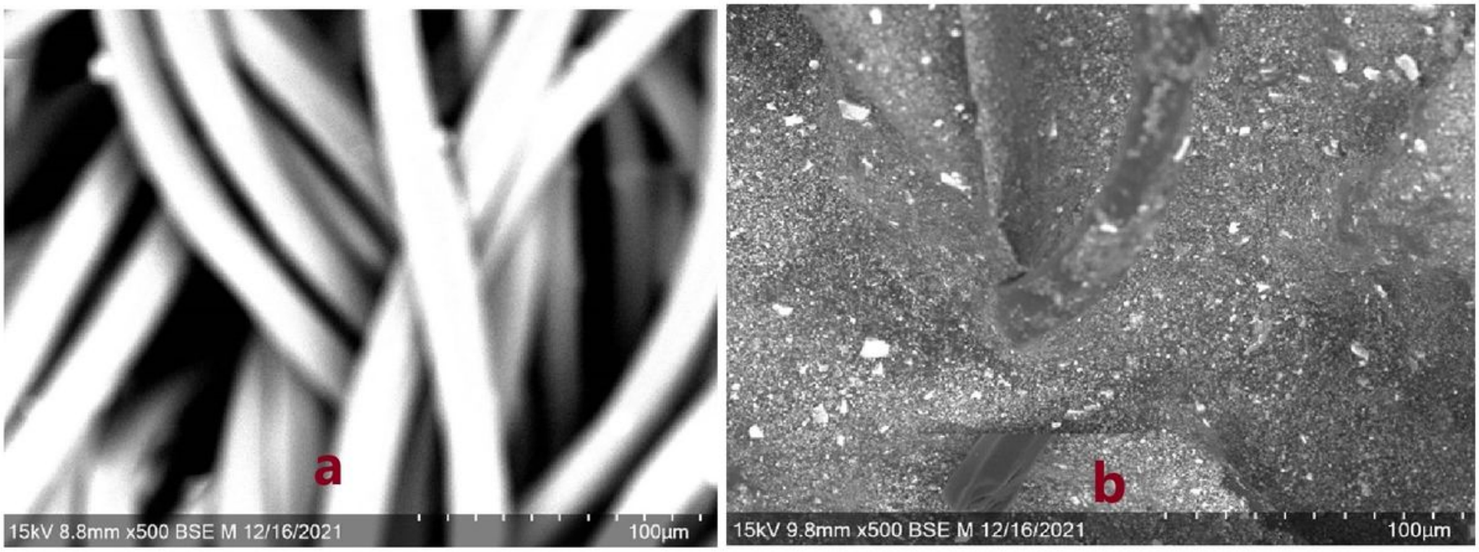

Figure 3

SEM image of uncoated PA-6,6 fabric (a) and SEM image of Cr oxide coated PA-6,6 fabric (b).

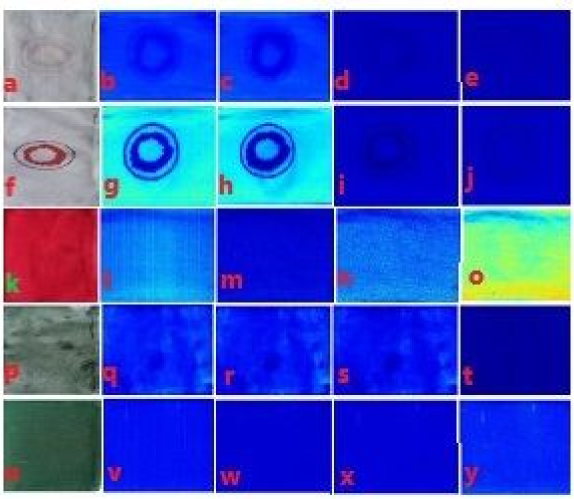

Figure 4

Comparison of Vis-HSI under different formulation of background and wavelength from 400 nm to 700 nm.

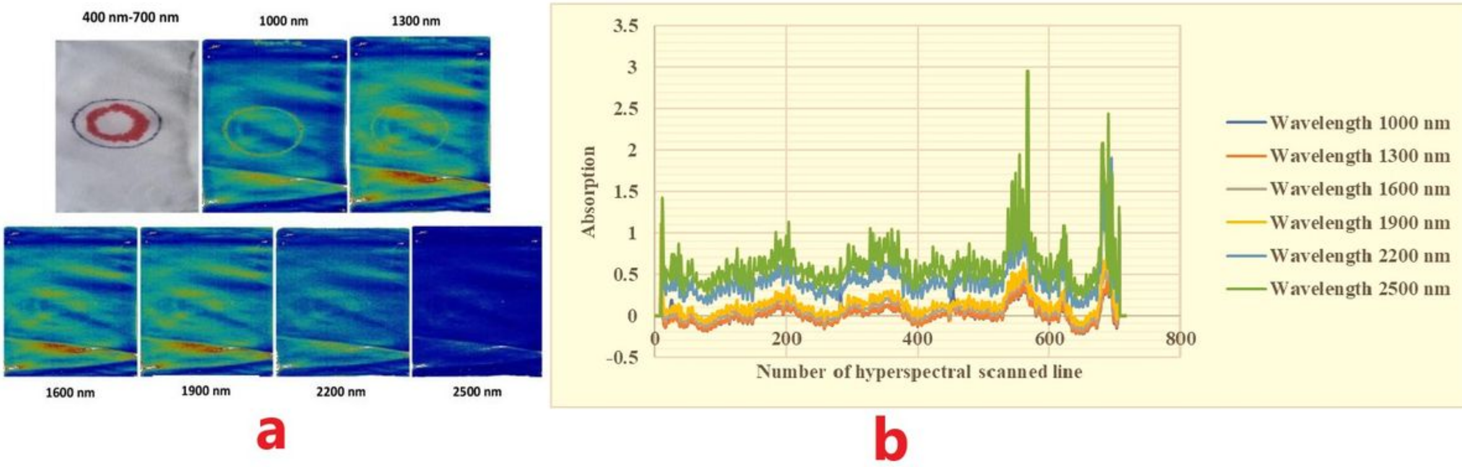

Figure 5

PA-6,6 fabric with black and red marked ‘circular area’ in front layer shown in 400-700 nm and scanned in IR-HSI, 1000-2500 nm.

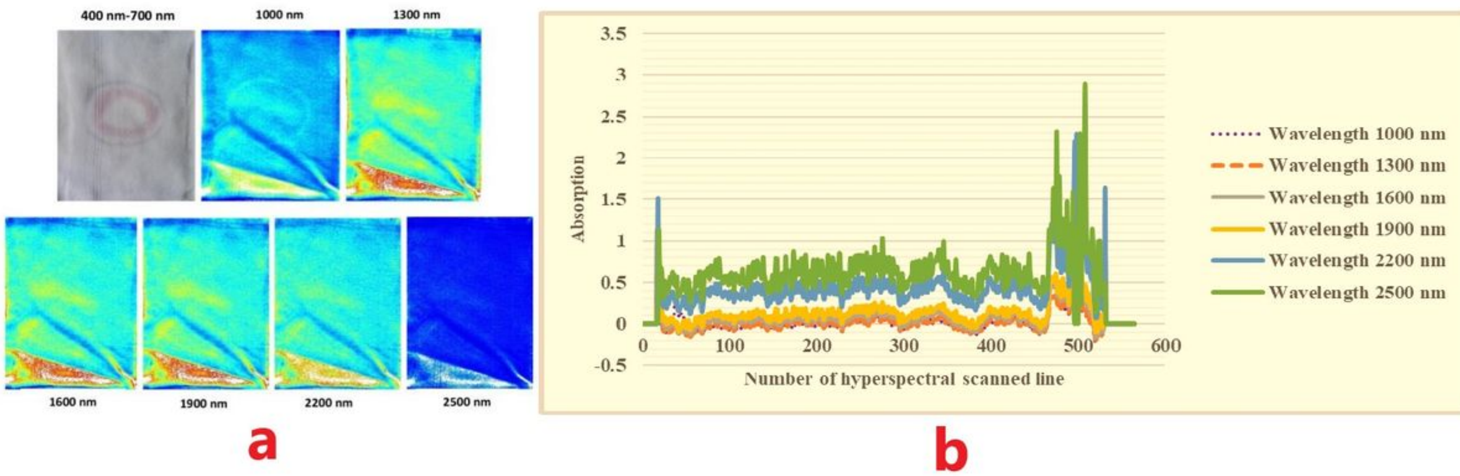

Figure 6

PA-6,6 fabric with black and red marked ‘circular area’ in back layer of fabric shown in 400-700 nm and scanned in IR-HSI, 1000-2500 nm.

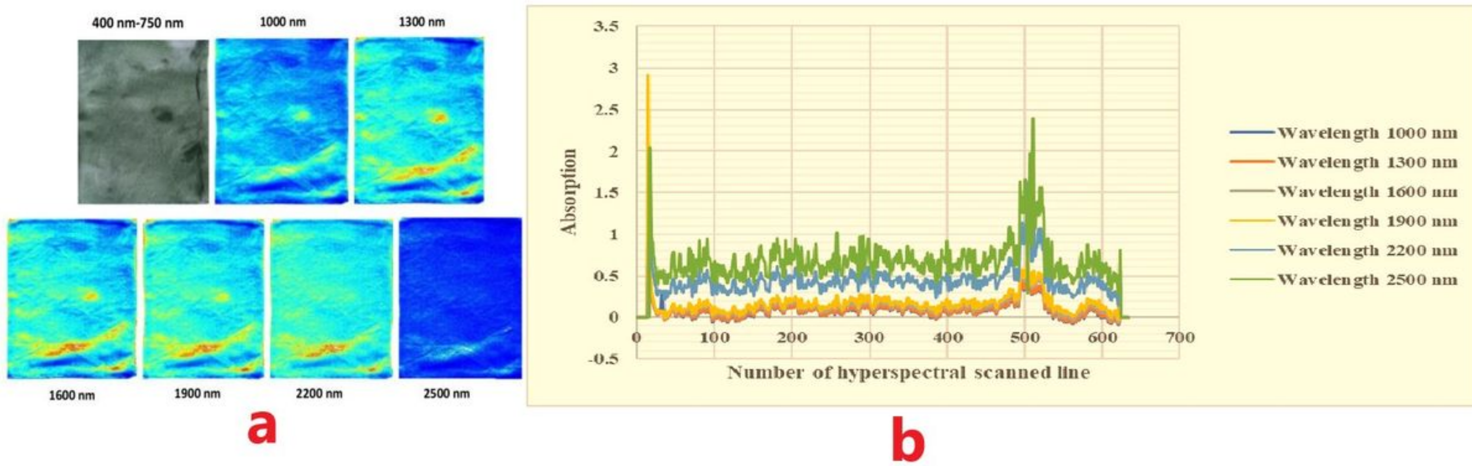

Figure 7

Cr oxide dyed PA-6,6 fabric with black and red marked ‘circular area’ in back layer of fabric shown in 400-700 nm and scanned in IR-HSI, 1000-2500 nm.

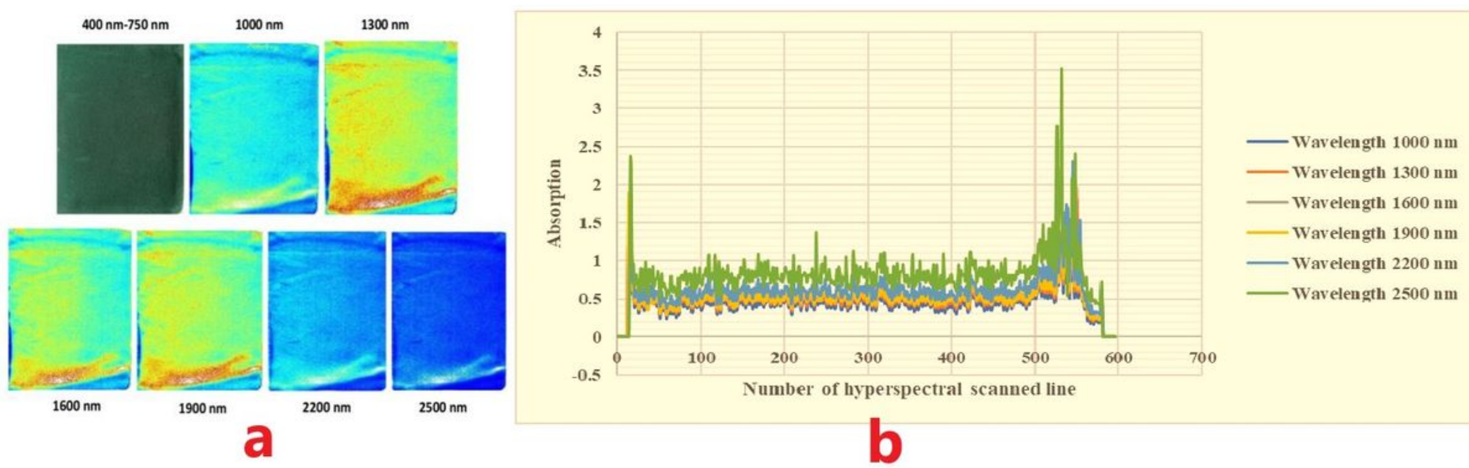

Figure 8

Cr oxide coated PA-6,6 fabric with black and red marked ‘circular area’ in back layer of fabric surface shown in 400-700 nm and scanned in IR-HSI, 1000-2500 nm.

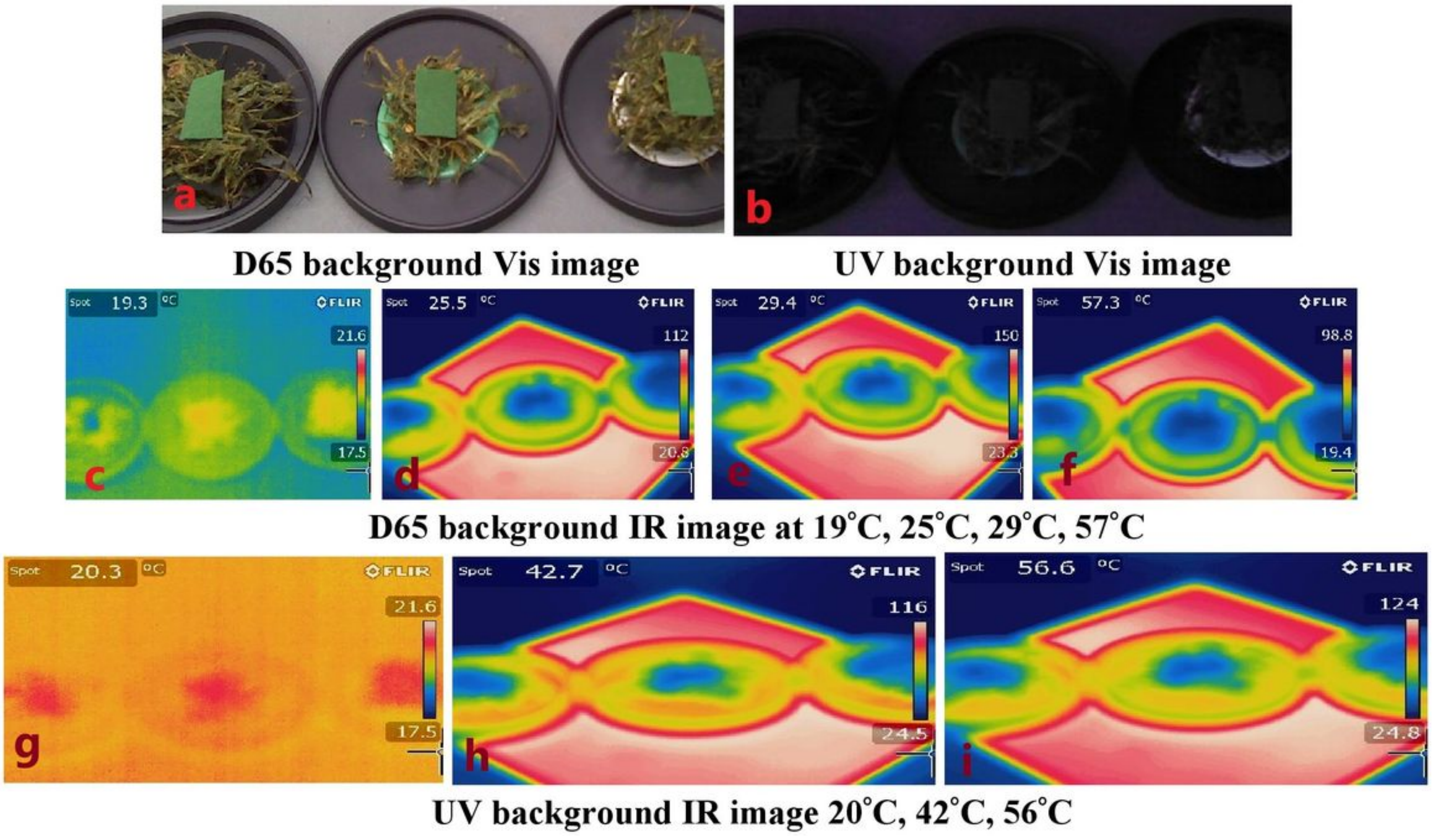

Figure 9

Cr oxide coated PA-6,6 fabric placed on woodland CB material, dry grass, *Bothriochloa Pertusa* in Vis-IR spectrum for CDRI assessment under D65 and UV lighting.

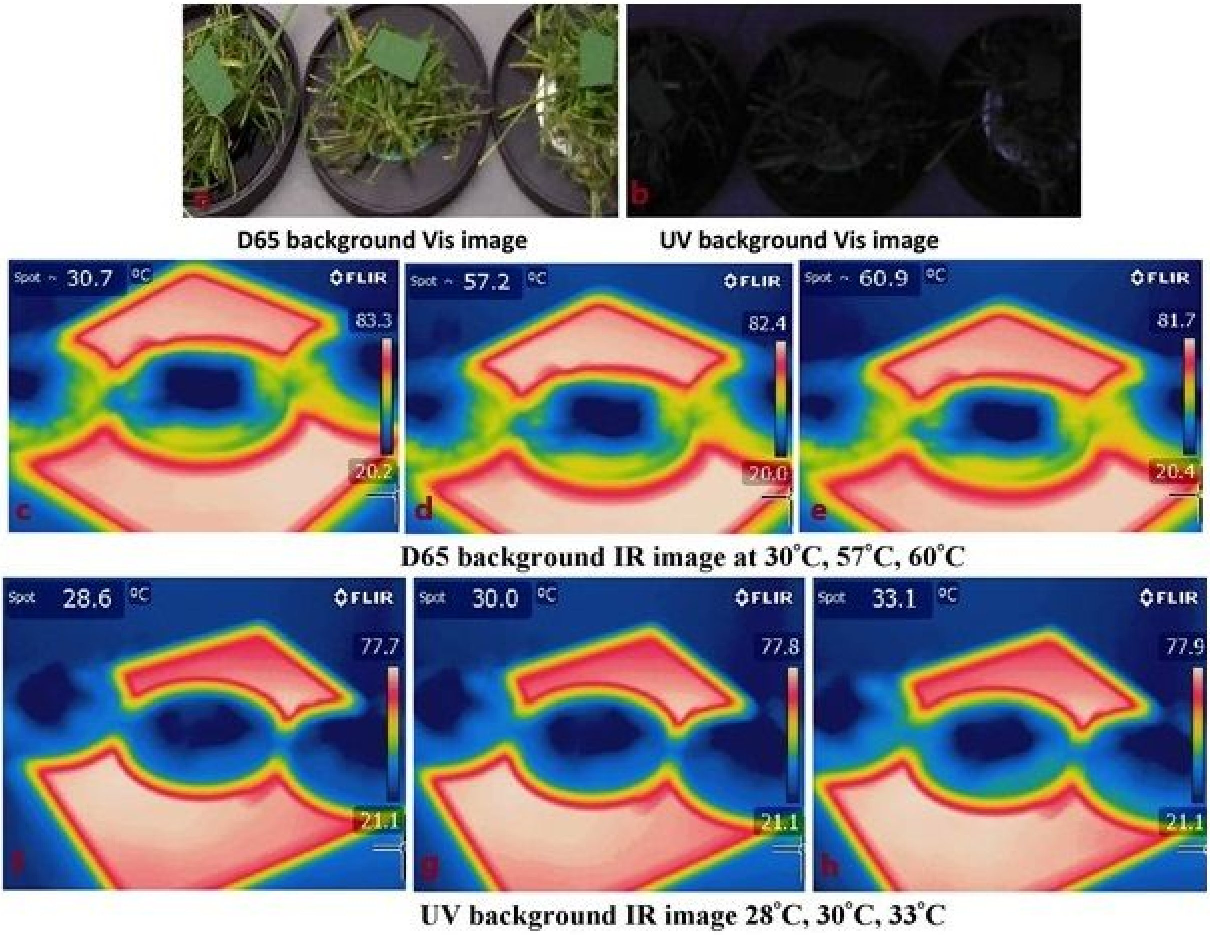

Figure 10

Cr oxide coated PA-6,6 fabric placed on woodland CB material, green grass, *Bothriochloa Pertusa* in Vis-IR spectrum for CDRI assessment from low to high temperature range at 28.6˚C, 30.0˚C, 30.7˚C, 33.1˚C, 57.2˚C, 60.9˚C under D65 and UV lighting.

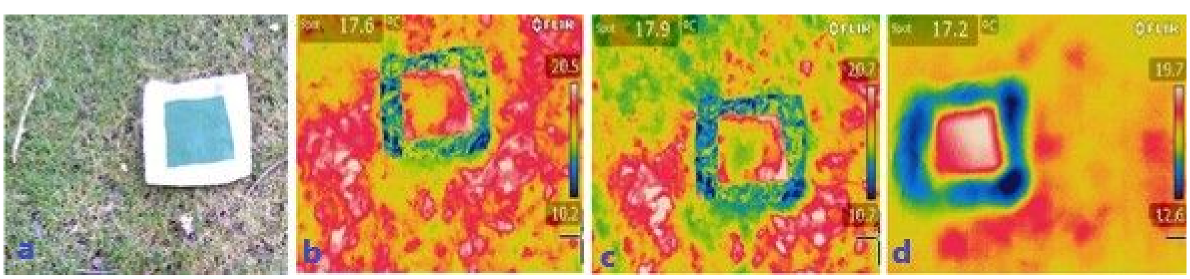

Figure 11

Cr oxide coated PA-6,6 fabric placed on Australian Grass (combined with dry grass and green grass), *Bothriochloa Pertusa*, captured by Vis-IR Camera at 17.6˚C, 17.2˚C, 17.9˚C under natural illumination, a sunny morning sunlight, 11 November, 2021.

Supplementary Files

This is a list of supplementary files associated with this preprint. Click to download.

- SupportinginformationTableSI1.pdf
- SupportinginformationTableSI10.pdf
- SupportinginformationTableSI11.pdf
- SupportinginformationTableSI12.pdf
- SupportinginformationTableSI13.pdf
- SupportinginformationTableSI14.pdf
- SupportinginformationTableSI15.pdf
- SupportinginformationTableSI16.pdf
- SupportinginformationTableSI17.pdf
- SupportinginformationTableSI18.pdf
- SupportinginformationTableSI19.pdf
- SupportinginformationTableSI2.pdf
- SupportinginformationTableSI20.pdf
- SupportinginformationTableSI21.pdf
- SupportinginformationTableSI22.pdf
- SupportinginformationTableSI23.pdf
- SupportinginformationTableSI24.pdf
- SupportinginformationTableSI25.pdf
- SupportinginformationTableSI3.pdf
- SupportinginformationTableSI4.pdf
- SupportinginformationTableSI5.pdf
- SupportinginformationTableSI6.pdf
- SupportinginformationTableSI7.pdf
- SupportinginformationTableSI8.pdf
- SupportinginformationTableSI9.pdf